

# A Practical Equation of State

Tarek Ahmed, SPE, Montana Tech

**Summary.** To use the Peng-Robinson equation of state (PREOS) to predict the phase and volumetric behavior of hydrocarbon mixtures, one needs to know the critical pressure,  $p_c$ , critical temperature,  $T_c$ , and acentric factor,  $\omega$ , for each component present in the mixture. For pure compounds, the required properties are well-defined, but nearly all naturally occurring gas and crude oil fluids contain some heavy fractions that are not well-defined and are not mixtures of discretely identified components. These heavy fractions often are lumped and called the "plus fraction" (e.g.,  $C_{7+}$  fraction). Adequately characterizing these undefined plus fractions in terms of their critical properties and acentric factors has long been a problem. Changing the characterization of the plus fraction can have a significant effect on the volumetric and phase behavior of a mixture predicted by the PREOS. This limitation of the PREOS results from an improper procedure of determining coefficients  $a$ ,  $b$ , and  $\alpha$  for the plus fraction and for hydrocarbon components with critical temperatures less than the system temperature (i.e., methane and nitrogen). This paper presents a practical approach to calculating the parameters of the PREOS for the undefined fractions to improve the predictive capability of the equation. Use of the modified equation is illustrated by matching laboratory data on several crude oil and gas-condensate systems.

## Introduction

An equation of state (EOS) is an analytical expression relating the pressure to the volume and temperature. The expression is used to describe the volumetric behavior, the vapor/liquid equilibria (VLE), and the thermal properties of pure substances and mixtures. Numerous EOS's have been proposed since van der Waals<sup>1</sup> introduced his expression in 1873. These equations were generally developed for pure fluids and then extended to mixtures through the use of mixing rules. The mixing rules are simply a means of calculating mixture parameters equivalent to those of a pure substance. The PREOS<sup>2</sup> is perhaps the most popular and widely used EOS. In terms of the molar volume  $V_m$ , they proposed the following two-constant cubic EOS:

$$p = [RT/(V_m - b)] - a(T)/[V_m(V_m + b) + b(V_m - b)]. \quad (1)$$

van der Waals observed that for a pure component, the first and second isothermal derivatives of pressure with respect to volume are equal to zero at the critical point of the substance. This observation can be expressed mathematically as

$$(\delta p / \delta V_m)_{T_c} = 0 \quad (2)$$

$$\text{and } (\delta^2 p / \delta V_m^2)_{T_c} = 0. \quad (3)$$

Peng and Robinson imposed the above derivative constraints on Eq. 1 and solved the resulting two expressions for the parameters  $a(T_c)$  and  $b$  to give

$$a(T_c) = \Omega_a (RT_c)^2 / p_c \quad (4)$$

$$\text{and } b = \Omega_b (RT_c) / p_c. \quad (5)$$

where the dimensionless parameters  $\Omega_a$  and  $\Omega_b$  are 0.45724 and 0.07780, respectively. At temperatures other than the  $T_c$ , Peng and Robinson adopted Soave's<sup>3</sup> approach for evaluating  $a(T)$ . The generalized expression for the temperature-dependent parameter is given by

$$a(T) = a(T_c) \alpha(T), \quad (6)$$

$$\text{where } \alpha(T) = \{1 + m[1 - (T/T_c)^{0.5}]\}^2, \quad (7)$$

$$\text{with } m = 0.3746 + 1.5423\omega - 0.2699\omega^2. \quad (8)$$

Introducing the compressibility factor,  $z$ , into Eq. 1 gives

$$z^3 + (B - 1)z^2 + (A - 3B^2 - 2B)z - (AB - B^2 - B^3) = 0, \quad (9)$$

$$\text{where } A = a(T)p/(RT)^2 \quad (10)$$

$$\text{and } B = bp/(RT). \quad (11)$$

To use Eq. 9 for mixtures, Peng and Robinson recommend the following classic mixing rules:

$$[a(T)]_{\text{mix}} = \sum_i \sum_j x_i x_j [a(T_{ci}) \alpha_i(T) \alpha_j(T)]^{0.5} (1 - k_{ij}) \quad (12)$$

$$\text{and } (b)_{\text{mix}} = \sum_i (x_i b_i). \quad (13)$$

In the application of Eqs. 12 and 13 to a hydrocarbon mixture,  $a(T)$  and  $b$  are calculated for each component in the mixture with Eqs. 4 through 8. Questionable assumptions are made in the application of these equations to the plus fraction and to hydrocarbon components with critical temperatures less than the system temperature. These assumptions (outlined below) provide the reasoning for the proposed modification of the popular EOS.

**Assumption 1.** In the derivation of expressions for  $a(T)$  and  $b$ , as represented by Eqs. 4 and 5, the critical isotherm of a component is assumed to have a slope of zero and an inflection point at the critical point. The assumption, described mathematically by Eqs. 2 and 3, is valid only for a pure component. Because the plus fraction lumps millions of compounds that are making up the fraction, it is unlikely that Eqs. 4 and 5 would provide an accurate representation of the attraction parameter  $a(T)$  and the covolume  $b$ .

**Assumption 2.** The coefficients of Eq. 7 were developed by regressing vapor-pressure data from the normal boiling point to the critical point for several pure components. Again, it is unlikely that this equation will suffice for the higher-molecular-weight plus fractions.

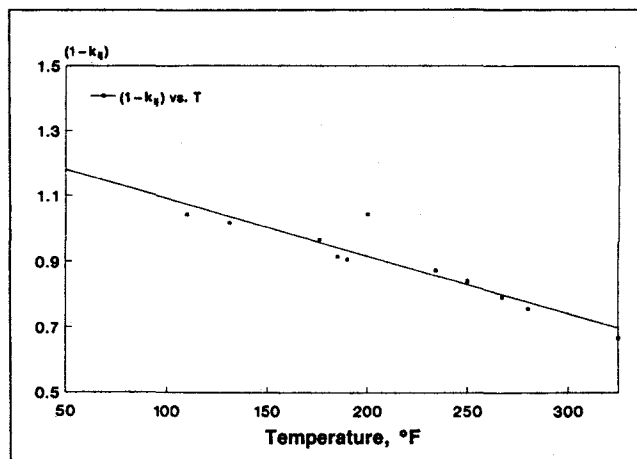
**Assumption 3.** As pointed out previously, the theoretical  $\Omega_a$  and  $\Omega_b$  values in the PREOS arise from imposing the van der Waals critical-point conditions, as expressed by Eqs. 2 and 3, on Eq. 1. These values essentially reflect satisfaction of pure-component density and vapor-pressure data below critical temperature. At reservoir conditions, methane and nitrogen in particular are well above their critical points. Coats and Smart<sup>4</sup> pointed out that no theory or clear-cut guide exists to selection or alteration of the  $\Omega$  for components well above their critical temperatures.

Wilson *et al.*<sup>5</sup> showed the distinct effect of the plus fraction's characterization procedure on all the PVT relationships predicted by an EOS. A number of studies<sup>4,6-10</sup> reported comparisons of EOS and laboratory PVT results for a wide variety of reservoir fluids and conditions; most of these studies emphasize the plus-fraction characterization as the key element in attaining agreement between EOS and laboratory results.

Coats and Smart<sup>4</sup> presented numerous examples of matching the measured and calculated data for nine reservoir fluids of various degrees of complexity. They observed that without regression or significant adjustment of EOS parameters, the PREOS will not adequately predict observed fluid PVT behavior. Coats and Smart indicated that the adjustment of five parameters in the PREOS is frequently necessary and sufficient for good data match. These parameters are  $\Omega_a$  and  $\Omega_b$  of methane,  $\Omega_a$  and  $\Omega_b$  of the plus fraction, and the methane plus fraction binary interaction coefficient. Whitson<sup>9</sup> observed that the method of adjusting the EOS constants

TABLE 1—COEFFICIENTS OF EQS. 16 AND 18

Coefficient	$a(T_c)$	$b$	$m$
$C_0$	$-2.433525 \times 10^7$	$-6.8453198$	$-36.91776$
$C_1$	$8.3201587 \times 10^3$	$1.730243 \times 10^{-2}$	$-5.2393763 \times 10^{-2}$
$C_2$	$-0.18444102 \times 10^2$	$-6.2055064 \times 10^{-6}$	$1.7316235 \times 10^{-2}$
$C_3$	$3.6003101 \times 10^{-2}$	$9.0910383 \times 10^{-9}$	$-1.3743308 \times 10^{-5}$
$C_4$	$3.4992796 \times 10^7$	$13.378898$	$12.718844$
$C_5$	$2.838756 \times 10^7$	$7.9492922$	$10.246122$
$C_6$	$-1.1325365 \times 10^7$	$-3.1779077$	$-7.6697942$
$C_7$	$6.418828 \times 10^6$	$1.7190311$	$-2.6078099$

Fig. 1—Optimum  $k_{11}$  between  $C_1$  and  $C_{7+}$  as a function of temperature.

$\Omega_a$  and  $\Omega_b$  for the plus fraction is essentially the same as altering the critical properties of the heavy fraction.

Several authors<sup>9,11-15</sup> showed that the ability of the EOS to predict the phase behavior of complex hydrocarbon mixtures can be substantially improved by splitting or breaking down the plus fraction into a manageable number of pseudocomponents for EOS calculations.

### Description of the Proposed Modification

Riazi and Daubert<sup>16</sup> developed a simple two-parameter equation for predicting the physical properties of pure compounds and undefined petroleum fractions. The proposed correlation is applicable in the molecular-weight range of 70 to 300 and normal boiling point range of 80 to 650°F. They proposed the following expression for the molecular-weight determination in terms of the boiling point and specific gravity of the substance:

$$M = a(T_b)^b \gamma^c \exp(dT_b + e\gamma + fT_b\gamma), \dots (14)$$

where  $a=581.960$ ,  $b=0.97476$ ,  $c=5.43076 \times 10^{-4}$ ,  $e=9.53384$ , and  $f=1.11056 \times 10^{-3}$ .

Because the inadequacy of the predictive capability of the PREOS lies with the three assumptions outlined, an approach was devised in this study to remove these assumptions. In the elimination of the first two assumptions, 49 hypothetical heavy petroleum fractions (i.e., plus fractions) with physical properties (density, molecular weight, and boiling point) governed by the applicability range of Eq. 14 were generated. The specific steps of the procedure are outlined below.

**Step 1.** Each hypothetical heavy fraction with a specified molecular weight, boiling point, and density (specific gravity) is subjected to 10 temperature and 10 pressure values in the range of 60 to 300°F and 14.7 to 7,000 psia. The specified density is then adjusted to account for the temperature and pressure increases. A total of 100 density values is generated for each hypothetical heavy fraction.

**Step 2.** Eq. 9 is rearranged and expressed in terms of the density to give

TABLE 2—COMPARISON OF PREDICTED OIL DENSITIES WITH EXPERIMENTAL DATA

	$p$ (psia)	$T$ (°F)	Density (g/cm <sup>3</sup> )			
			Exp.	S-K	A-K	EOS
<b>S-K Data</b>						
A-1	3,185	120	0.696	0.729	0.720	0.718
A-2	5,270	120	0.745	0.759	0.736	0.745
A-3	8,220	120	0.814	0.817	0.773	0.802
A-4	1,600	120	0.702	0.712	0.701	0.718
B-1	2,915	250	0.697	0.702	0.688	0.663
C-1	2,880	120	0.652	0.655	0.642	0.663
C-2	1,010	120	0.716	0.724	0.712	0.732
C-3	5,330	120	0.712	0.685	0.672	0.712
D-1	4,330	120	0.731	0.729	0.714	0.726
E-1	4,195	120	0.753	0.744	0.728	0.748
F-1	3,185	250	0.654	0.670	0.658	0.638
F-2	4,315	250	0.657	0.664	0.656	0.628
F-3	5,330	250	0.677	0.684	0.672	0.648
G-2	3,485	35	0.679	0.675	0.667	0.701
G-3	4,970	35	0.766	0.764	0.748	0.764
<b>C-S Data</b>						
Oil 1	2,520	180	0.768	0.784	0.762	0.764
Oil 2	4,460	176	0.530	0.509	0.537	0.544
Oil 3	2,115	140	0.736	0.807	0.809	0.752
Oil 3	2,362	160	0.722	0.804	0.796	0.726
Oil 3	2,597	180	0.708	0.795	0.785	0.701
Oil 3	2,792	200	0.695	0.788	0.772	0.683
Oil 4	2,547	250	0.646	0.647	0.651	0.615
Oil 4	2,283	180	0.679	0.679	0.682	0.672
Oil 4	1,958	110	0.711	0.709	0.712	0.719
Oil 6	2,746	234	0.609	0.620	0.623	0.599
Oil 7	1,694	131	0.713	0.717	0.735	0.722
Average absolute error, %				6.58	6.69	5.58

$$[a(T_c)\alpha(T)b - RTb^2 - pb^3] \rho^3 - M[a(T_c)\alpha(T) - 3pb^2 - 2RTb] \rho^2 - M^2(pb - RT) \rho - pM^3 = 0. \dots (15)$$

**Step 3.** Eq. 15 is incorporated into a nonlinear regression model that uses  $a(T_c)$ ,  $b$ , and  $\alpha(T)$  as regression variables. For each hypothetical heavy fraction under consideration, Eq. 15 is solved for the density by optimizing the regression variables to match the fraction generated density data.

**Step 4.** The optimized regression variables [i.e.,  $a(T_c)$ ,  $b$ , and  $\alpha(T)$ ] are correlated with  $M$ ,  $\gamma$ , or  $T$  by the following relationships. For  $a(T_c)$  or  $b$  of the plus fraction,

$$a(T_c) \text{ or } b = \left[ \sum_{i=0}^3 (C_i D^i) \right] + C_4/D + \left[ \sum_{i=5}^6 (C_i \gamma^{i-4}) \right] + C_7/\gamma, \dots (16)$$

with  $D = (M/\gamma)_{c+}$ . Table 1 gives values of  $C_0$  through  $C_7$  [for  $a(T_c)$  and  $b$ ] of the above expression. For  $\alpha(T)$ , the Peng and Robinson  $\alpha(T)$  function as expressed by Eq. 7 is modified according to

$$\alpha(T) = \{1 + m[1 - (520/T)^{0.5}]\}^2, \dots (17)$$

TABLE 3—COATS AND SMART COMPOSITIONAL DATA

	Gas 2*	Gas 2**	Gas 5	Oil 1	Oil 2	Oil 3	Oil 4	Oil 6	Oil 7
CO <sub>2</sub>	0.00690	0.00610	0.02170	0.00440	0.00900	0.60310	0.02350	0.01030	0.0008
N <sub>2</sub>		0.00420	0.00340	0.00450	0.00300	0.00930	0.00110	0.00550	0.0164
H <sub>2</sub> S	0.00040	0.00040							
C <sub>1</sub>	0.58320	0.57490	0.70640	0.35050	0.53470	0.07050	0.35210	0.36470	0.2840
C <sub>2</sub>	0.13550	0.13450	0.10760	0.04640	0.11460	0.01570	0.06720	0.09330	0.0716
C <sub>3</sub>	0.07610	0.07520	0.04940	0.02460	0.08790	0.03060	0.06240	0.08850	0.1048
C <sub>4</sub>	0.04030	0.04150	0.03020	0.01660	0.04560	0.03310	0.05070	0.06000	0.0840
C <sub>5</sub>	0.02410	0.02330	0.01350	0.01600	0.02090	0.02680	0.05230	0.03780	0.0382
C <sub>6</sub>	0.01900	0.01790	0.00900	0.05460	0.01510	0.02580	0.04100	0.03560	0.0405
C <sub>7+</sub>	0.11450	0.12200	0.05880	0.48240	0.16920	0.18510	0.34970	0.30430	0.3597
M <sub>+</sub>	193	193	153	225	173	189	213	200	252
γ <sub>+</sub>	0.8135	0.8115	0.8100	0.9000	0.8364	0.8275	0.8405	0.8366	0.8429
T <sub>i</sub> , °F	190	190	267	180	176	179	250	234	131
p, psig	4,450	4,415	4,842	2,520	4,460	2,597	2,547	2,746	1,694

TABLE 4—BINARY INTERACTION COEFFICIENTS FOR GAS 2\*

Component i	Component j										
	CO <sub>2</sub>	N <sub>2</sub>	C <sub>1</sub>	C <sub>2</sub>	C <sub>3</sub>	i-C <sub>4</sub>	n-C <sub>4</sub>	i-C <sub>5</sub>	n-C <sub>5</sub>	C <sub>6</sub>	C <sub>7+</sub>
CO <sub>2</sub>	0.000	0.012	0.100	0.100	0.100	0.100	0.100	0.100	0.100	0.100	0.100
N <sub>2</sub>		0.000	0.100	0.100	0.100	0.100	0.100	0.100	0.100	0.100	0.100
C <sub>1</sub>			0.000	0.000	0.000	0.000	0.000	0.000	0.000	0.001	0.061
C <sub>2</sub>				0.000	0.000	0.000	0.000	0.000	0.000	0.001	0.049
C <sub>3</sub>					0.000	0.000	0.000	0.000	0.000	0.001	0.039
i-C <sub>4</sub>						0.000	0.000	0.000	0.000	0.000	0.031
n-C <sub>4</sub>							0.000	0.000	0.000	0.000	0.025
i-C <sub>5</sub>								0.000	0.000	0.000	0.020
n-C <sub>5</sub>									0.000	0.000	0.016
C <sub>6</sub>										0.000	0.013
C <sub>7+</sub>											0.000

$$\text{with } m = [D/(C_0 + C_1 D)] + C_2 M + C_3 M^2 + C_4/M + C_5 \gamma + C_6 \gamma^2 + C_7/\gamma. \quad (18)$$

Table 1 includes the values  $C_0$  through  $C_7$  for Eq. 18.

In the elimination of the third assumption, the Peng and Robinson parameters [i.e.,  $a(T_c)$ ,  $b$ , and  $m$ ] for methane and nitrogen are altered. For this approach, 100  $z$ -factor values for each component were obtained from appropriate gas-compressibility-factor charts.  $a(T_c)$ ,  $b$ , and  $m$  (to be used in Eq. 17) for methane and nitrogen were optimized by incorporating a regression model in solving Eq. 9 and matching the  $z$ -factor data for each fraction. The optimized values are  $a(T_c) = 4,569.3589$ ,  $b = 0.46825820$ , and  $m = -0.97962859$  for nitrogen and  $a(T_c) = 7,709.7080$ ,  $b = 0.46749727$ , and  $m = -0.54976500$  for methane.

Several computational schemes<sup>7,10,17</sup> for generating binary interaction coefficients were tested for the purpose of providing the modified PREOS with a systematic and consistent procedure for

determining the  $k_{ij}$ . Petersen's<sup>17</sup> computational technique was adopted and appropriately modified to provide the proper EOS coefficients. The technique is described in the following steps.

**Step 1.** Set  $k_{\text{CO}_2-\text{N}_2} = 0.12$ ,  $k_{\text{CO}_2-\text{hydrocarbons}} = 0.10$ , and  $k_{\text{N}_2-\text{hydrocarbons}} = 0.10$ .

**Step 2.** Estimate the binary interaction coefficient between methane and the plus fraction,  $k_{\text{C}_1-\text{C}_+}$ . To provide this estimate, the coefficient under consideration was adjusted to minimize the error in calculating the saturation pressures of 12 hydrocarbon mixtures. Results of the study (Fig. 1) indicate the strong dependency of the calculated optimum values of  $k_{\text{C}_1-\text{C}_+}$  on system temperatures. The following linear relationship provides an appropriate estimate of the parameter:

$$k_{\text{C}_1-\text{C}_+} = 0.00189T - 0.297659, \quad (19)$$

where  $T$  = system temperature in degrees Fahrenheit.

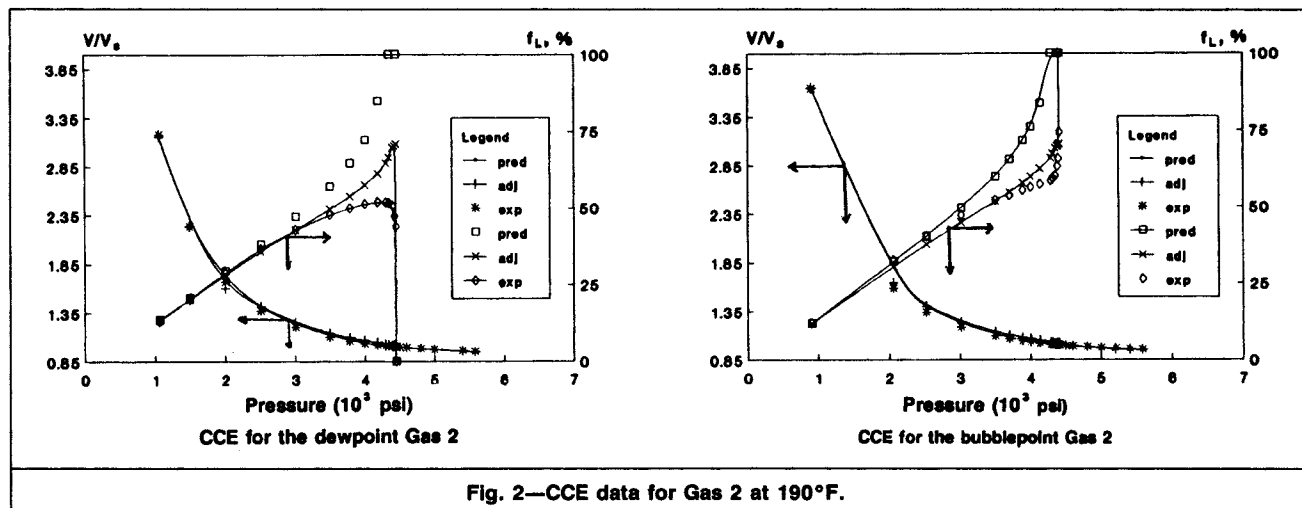


Fig. 2—CCE data for Gas 2 at 190°F.

TABLE 5—CVE AT 190°F FOR DEWPOINT GAS

Component	Pressure (psig)						
	4,450.0	3,500.0	2,700.0	1,900.0	1,100.0	500.0	500*
CO <sub>2</sub>	0.00730	0.00767	0.00790	0.00824	0.00874	0.00922	0.00228
N <sub>2</sub>	0.00000	0.00000	0.00000	0.00000	0.00000	0.00000	0.00000
C <sub>1</sub>	0.58320	0.71198	0.72463	0.72791	0.71235	0.65973	0.07116
C <sub>2</sub>	0.13550	0.13745	0.13945	0.14384	0.15417	0.17230	0.06429
C <sub>3</sub>	0.07610	0.06804	0.06713	0.06782	0.07388	0.09265	0.07722
i-C <sub>4</sub>	0.02015	0.01640	0.01568	0.01528	0.01625	0.02135	0.03199
n-C <sub>4</sub>	0.02015	0.01538	0.01447	0.01387	0.01463	0.01961	0.03818
i-C <sub>5</sub>	0.01205	0.00822	0.00738	0.00666	0.00658	0.00874	0.03124
n-C <sub>5</sub>	0.01205	0.00783	0.00691	0.00611	0.00592	0.00781	0.03397
C <sub>6</sub>	0.01900	0.01069	0.00885	0.00719	0.00631	0.00786	0.06607
C <sub>7+</sub>	0.11450	0.01634	0.00762	0.00308	0.00117	0.00073	0.58360

z Factor							
Adjusted	0.9805	0.8359	0.8016	0.8031	0.8461	0.9061	
Experimental	0.9969	0.8402	0.7966	0.8140	0.8603	0.9108	
Predicted	0.9767	0.8307	0.7994	0.8026	0.8459	0.9059	

G <sub>p</sub> (%)							
Adjusted	0.00000	12.89401	25.41145	41.00742	58.98976	73.30406	
Experimental	0.00000	9.589	22.551	39.165	58.225	72.743	
Predicted	0.00000	11.008	24.146	40.224	58.643	73.215	

Liquid Dropout (%)							
Adjusted	0.0	56.52650	50.99886	46.20221	41.35549	37.25255	
Experimental	0.0	52.31	49.40	45.33	40.51	36.82	
Predicted	0.0	63.77	54.13	47.64	41.90	37.43	

\*Residual liquid composition.

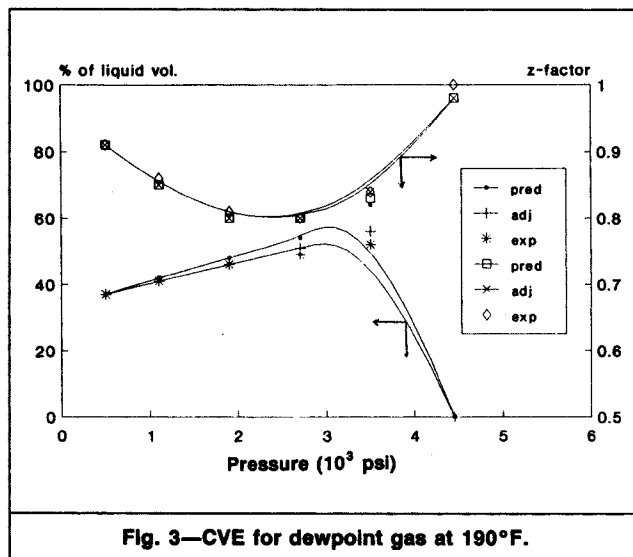


Fig. 3—CVE for dewpoint gas at 190°F.

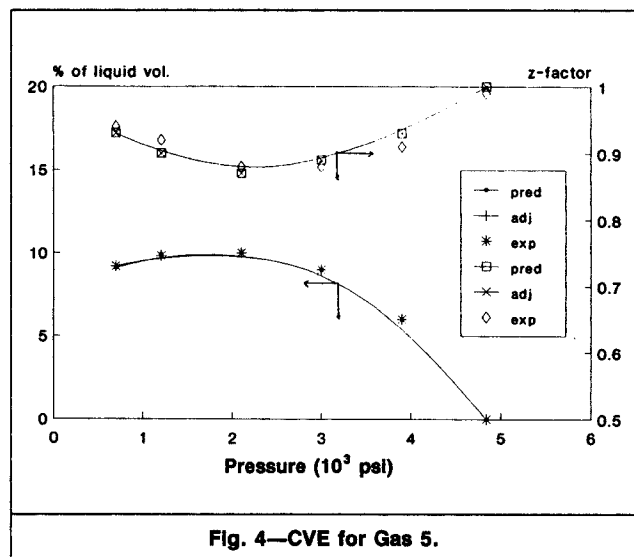


Fig. 4—CVE for Gas 5.

Step 3. Calculate the binary interaction coefficients between components heavier than methane (i.e., C<sub>2</sub>, C<sub>3</sub>...etc.) and the plus fraction according to the following expression:<sup>17</sup>

$$k_{C_n-C_+} = 0.8k_{C_{(n-1)}-C_+}, \dots \dots \dots (20)$$

where  $n$  = number of carbon atoms.

Step 4. Determine the remaining  $k_{ij}$  from<sup>17</sup>

$$k_{ij} = k_{i-C_+} [(M_j)^5 - (M_i)^5] / [(M_{C_+})^5 - (M_i)^5], \dots \dots \dots (21)$$

#### Application of the Modified EOS

To validate the proposed modification, the modified EOS was used

to simulate a variety of laboratory tests and to compare the simulated results and actual data. For convenience and brevity, several terms presented and defined by Coats and Smart<sup>4</sup> are adopted in the study. "Predicted" denotes the simulated results calculated by the EOS without altering any of the equation parameters. "Adjusted" refers to EOS results calculated after the binary interaction coefficient between methane and the plus fraction is adjusted to match the saturation pressure of the hydrocarbon system. The constant-composition, constant-volume, and differential expansions are referred to as CCE, CVE, and DE, respectively.  $G_p$  = cumulative gas removed from a laboratory CVE cell,  $f_L$  = liquid volume

TABLE 6—EXPANSION DATA FOR GAS 5

Component	Pressure (psig)						
	4,842.0	3,900.0	3,000.0	2,100.0	1,200.0	700.0	700.0*
CO <sub>2</sub>	0.02170	0.02185	0.02207	0.02237	0.02276	0.02302	0.00611
N <sub>2</sub>	0.00340	0.00348	0.00355	0.00359	0.00360	0.00356	0.00032
C <sub>1</sub>	0.70640	0.72207	0.73481	0.74357	0.74575	0.73990	0.08684
C <sub>2</sub>	0.10760	0.10893	0.11010	0.11124	0.11256	0.11352	0.02989
C <sub>3</sub>	0.04940	0.04957	0.04970	0.04997	0.05083	0.05216	0.02532
i-C <sub>4</sub>	0.01510	0.01502	0.01493	0.01491	0.01518	0.01583	0.01246
n-C <sub>4</sub>	0.01510	0.01490	0.01471	0.01460	0.01490	0.01574	0.01636
i-C <sub>5</sub>	0.00675	0.00658	0.00639	0.00625	0.00633	0.00681	0.01184
n-C <sub>5</sub>	0.00675	0.00653	0.00629	0.00610	0.00615	0.00668	0.01428
C <sub>6</sub>	0.00900	0.00853	0.00802	0.00753	0.00741	0.00814	0.03040
C <sub>7+</sub>	0.05880	0.04254	0.02942	0.01986	0.01452	0.01467	0.76619
z Factor							
Adjusted	1.0085	0.9324	0.8870	0.8742	0.8990	0.9290	
Experimental	0.985	0.911	0.881	0.882	0.916	0.943	
Predicted	1.0082	0.9320	0.8867	0.8740	0.8989	0.9290	
G <sub>p</sub> (%)							
Adjusted	0.00000	13.373	29.34	48.29	69.02	80.561	
Experimental	0.00000	12.812	29.341	49.110	69.907	81.220	
Predicted	0.00000	13.334	29.320	48.295	69.034	80.575	
Liquid Dropout (%)							
Adjusted	0.0	6.37	9.24	10.19	9.84	9.20	
Experimental	0.0	6.10	9.10	10.40	9.90	9.10	
Predicted	0.0	6.20	9.18	10.15	9.80	9.17	

\*Residual liquid composition.

divided by cell volume during expansion,  $V/V_s$  = total volume of the hydrocarbon system at any given pressure divided by the volume of the mixture at saturation pressure,  $B_o$  = oil FVF in barrels at indicated pressure and temperature per barrel of residual oil at 60°F, and  $R_s$  = solution GOR, defined as the cubic feet of gas at 60°F and 14.7 psia per barrel of residual oil at standard conditions.

**Density Predictions.** To test the modified PREOS for its ability to predict the density of complex hydrocarbon mixtures under a wide range of pressures and temperatures, the equation was applied to predict densities of the 15 hydrocarbon mixtures used by Standing and Katz<sup>18</sup> to develop their popular correlation and the densities of 11 crude oil systems reported by Coats and Smart.<sup>4</sup> Table 2 summarizes results of the model and compares the predicted densities with those calculated from the Standing-Katz<sup>18</sup> (S-K) and Alani-Kennedy<sup>19</sup> (A-K) density correlations. In terms of the overall average absolute deviation, the modified EOS predicted the density of the 26 mixtures with the lowest deviation of 5.58%, which compares favorably with the two density correlations.

**Coats-Smart Hydrocarbon Systems.** Coats and Smart<sup>4</sup> reported a detailed experimental description of several hydrocarbon systems. Nine of the hydrocarbon systems, with the compositions given in Table 3, were used in the study. Results of the application of the modified PREOS to the selected hydrocarbon systems are presented below.

**Near-Critical Gas Systems.** Gas 2 is a near-critical gas-condensate fluid at a reservoir temperature of 190°F. Coats and Smart stated that because of the possibility of a small error in gas measurement

TABLE 7—CCE FOR OIL 1 AT 180°F

p (psig)	V/V <sub>s</sub>		
	Predicted	Adjusted	Experimental
5,000	0.9740	0.9739	0.9782
4,000	0.9832	0.9831	0.9862
3,000	0.9940	0.9940	0.9951
2,900	0.9952	0.9952	0.9961
2,800	0.9964	0.9964	0.9971
2,700	0.9977	0.9977	0.9982
2,600	0.9990	0.9990	0.9992
2,520	1.0000	1.0000	1.0000

during well testing, two slightly different separator gas/liquid ratios are used to obtain the two reservoir fluid compositions given in Table 3. The first sample (Gas 2\*) exhibited a saturation pressure and density of 4,465 psia and 28.85 lbm/ft<sup>3</sup> and was labeled a dewpoint gas. The second sample (Gas 2\*\*) displayed a bubblepoint of 4,430 psia and a density of 29.54 lbm/ft<sup>3</sup> and consequently was labeled a bubblepoint gas. In applying the modified expression to simulate the volumetric behavior of the two systems, Eqs. 19 through 21 initially were used to determine the binary interaction coefficients for each system. Table 4 lists these values for Gas 2\*. The modified equation predicts a dewpoint pressure of 3,890 psia (compared with 3,680 psia for the original PREOS) and a saturation density of 28.45 lbm/ft<sup>3</sup>. For the bubblepoint gas, the equation predicts a saturation pressure of 3,824 psia (the original PREOS predicts 3,664 psia) and a saturation density of 28.86 lbm/ft<sup>3</sup>.

TABLE 8—OBSERVED AND PREDICTED DATA, CRUDE OIL 2

Approach	$p_b$ (psia)	$R_s$ (scf/STB)	$B_{ob}$ (RB/STB)	$\rho$ (lbm/ft <sup>3</sup> )
Experimental	4,475	3,377	2.921	33.10
Coats-Smart	3,344 (-25.3)	2,550 (-25)	2.419 (-17)	31.10 (-6.0)
Modified EOS	4,502 (0.60)	3,019 (-7.9)	2.675 (-8.4)	33.99 (2.6)

Numbers in parentheses represent percent error of predictions.

TABLE 9—EXPANSION DATA FOR OIL 2

DE at 176°F						
p (psig)	$R_s$ (scf/STB)			$B_{ob}$ (RB/STB)		
	Predicted	Adjusted	Experimental	Predicted	Adjusted	Experimental
4,460.0	3,109.3	3,108	3,377	2.6746	2.6736	2.921
4,000.0	2,371.6	2,401	2,351	2.2875	2.3039	2.343
3,492.0	1,890.4	1,909	1,814	2.0460	2.0563	2.059
3,003.0	1,528.5	1,540	1,471	1.8673	1.8737	1.886
2,514.0	1,246.8	1,254	1,205	1.7309	1.7351	1.756
2,004.0	998.9	1,004	970	1.6119	1.6145	1.645
1,534.0	801.5	805	775	1.5174	1.5191	1.555
1,001.0	598.2	600	573	1.4192	1.4201	1.464
505.0	408.7	409	383	1.3240	1.3243	1.372
209.0	271.3	271	245	1.2489	1.2490	1.298
0.0	0.0	000	000	1.0601	1.0601	1.057

CVE AT 176°F							
Component	Pressure (psig)						
	4,460.0	3,600.0	2,800.0	2,000.0	1,200.0	600.0	600.0*
CO <sub>2</sub>	0.00900	0.00984	0.01020	0.01074	0.01158	0.01256	0.00352
N <sub>2</sub>	0.00300	0.00491	0.00479	0.00454	0.00405	0.00333	0.00020
C <sub>1</sub>	0.53470	0.73509	0.74529	0.74678	0.73019	0.67668	0.08654
C <sub>2</sub>	0.11460	0.11526	0.11767	0.12251	0.13386	0.15557	0.06976
C <sub>3</sub>	0.08790	0.07183	0.07101	0.07187	0.07858	0.10006	0.10309
i-C <sub>4</sub>	0.02280	0.01624	0.01548	0.01498	0.01568	0.02010	0.03705
n-C <sub>4</sub>	0.02280	0.01474	0.01381	0.01311	0.01351	0.01739	0.04213
i-C <sub>5</sub>	0.01045	0.00578	0.00514	0.00457	0.00434	0.00533	0.02363
n-C <sub>5</sub>	0.01045	0.00541	0.00473	0.00411	0.00381	0.00461	0.02492
C <sub>6</sub>	0.01510	0.00643	0.00526	0.00419	0.00348	0.00388	0.04092
C <sub>7+</sub>	0.16920	0.01447	0.00662	0.00260	0.00092	0.00050	0.56822

Deviation Factors						
Predicted	0.8391	0.8052	0.8011	0.8361	0.8899	
Adjusted	0.8388	0.8051	0.8011	0.8361	0.8899	
Experimental	0.798	0.783	0.788	0.843	0.913	

$G_p$ (%)						
Predicted	0.00000	9.08623	19.92349	33.48568	49.6732	63.18673
Adjusted	0.00000	8.95470	19.82727	33.42198	49.6384	63.17171
Experimental	0.00000	7.535	17.932	32.371	49.908	63.967

\*Residual liquid composition.

Fig. 2 compares experimental CCE data with the predicted and adjusted values for both systems. In simulating the test for the dew-point gas, the model predicts a bubblepoint system when the fluid is flashed just below the dewpoint pressure. With adjustment, the expression overestimates the liquid volume at higher pressures. The predicted and adjusted CVE results for the dewpoint gas are given in Table 5 and illustrated graphically in terms of liquid dropout

in Fig. 3. The match between the observed and adjusted data is excellent. The modified expression gives an average absolute error deviation of 3.3% for the liquid dropout after adjustment. In terms of the  $z$  factor, the equation predicts the data with an average error of 1.19% before adjustment and a deviation of 1.05% after adjustment. A detailed documentation of results of the proposed EOS for simulating CCE tests is given in Ref. 20.

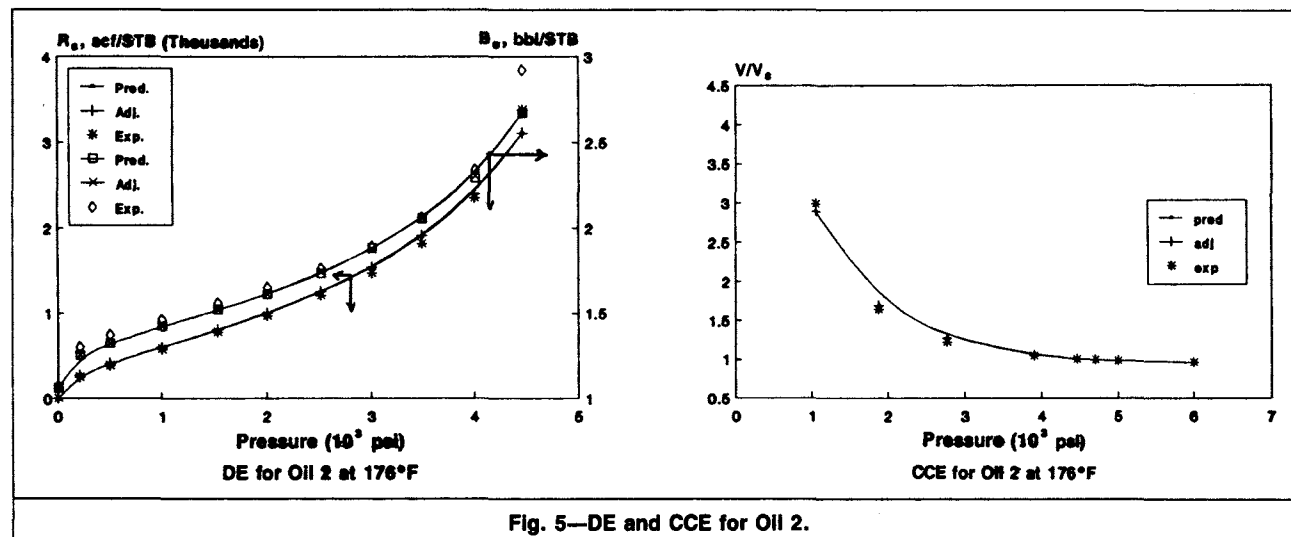


Fig. 5—DE and CCE for Oil 2.

**TABLE 10—OBSERVED AND PREDICTED DATA, CRUDE OIL 3**

	Temperature (°F)			
	140	160	180	200
Exp.				
$p_b$	2,144	2,392	2,627	2,821
$\rho_{ob}$	45.9	45.1	44.2	43.3
C-S				
$p_b$	1,776 (-17)	2,000 (-16.5)	2,210 (-16)	2,403 (-14.9)
$\rho_{ob}$	43.1 (-6)	42.3 (-6.2)	41.5 (-6.1)	40.6 (-6.2)
Mod. EOS				
$p_b$	2,082 (-2)	2,210 (-7.0)	2,304 (-12)	2,375 (-15.3)
$\rho_{ob}$	46.9 (2.2)	45.3 (0.5)	43.7 (-1.1)	41.8 (-3.4)

Numbers in parentheses represent percent error of predictions.

**Gas-Condensate System 5.** Gas 5 is a retrograde gas with a reported upper dewpoint pressure of 4,857 psia at 276°F. The model predicts an excellent value of 4,805 psia for the dewpoint pressure. On the basis of the original PREOS, the Coats-Smart model predicts a saturation pressure of 4,494 psia. In simulating the CVE and CCE tests for the system, the modified equation shows excellent predictive capabilities in reproducing the experimental data, as Table 6 illustrates. The tabulated results compare the observed data with the predicted and adjusted values in terms of  $z$  factor, liquid dropout,  $G_p$ ,  $V/V_s$ , and  $f_L$ . The predicted and adjusted values are essentially identical. The modified expression gives average deviations of 1.6% for the  $z$  factor, 1.3% for  $G_p$ , and 1.9%

**TABLE 11—OBSERVED AND PREDICTED DATA, CRUDE OIL 4**

	Temperature (°F)		
	110	180	250
Exp.			
$p_b$	1,988	2,313	2,577
$R_s$	701		932
$B_{ob}$	1.341		1.671
$\rho_{ob}$	44.4	42.4	40.3
C-S			
$p_b$	1,694 (-14.8)	2,033 (-12.1)	2,274 (-11.76)
$R_s$	611 (-12.8)		756 (-18.9)
$B_{ob}$	1.294 (-3.5)		1.517 (-9.2)
$\rho_{ob}$	40.0 (-9.9)	38.4 (9.4)	36.8 (-8.7)
Mod. EOS			
$p_b$	1,695 (-14.7)	2,330 (0.7)	2,655 (3.0)
$R_s$	694 (-0.9)		949 (1.8)
$B_{ob}$	1.323 (-1.3)		1.769 (5.9)
$\rho_{ob}$	44.8 (1.1)	41.96 (-1.0)	38.35 (-4.8)

Numbers in parentheses represent percent error of the predictions.

for liquid dropout. The near-exact match with reported data is documented in Fig. 4.

**Crude Oil 1.** This oil, with the composition given in Table 3, exhibits a saturation pressure and density of 2,535 psia and 47.96 lbm/ft<sup>3</sup> at 180°F. The model predicted excellent values for the bubblepoint pressure and saturation density of 2,501 psia and 47.68 lbm/ft<sup>3</sup>. The modified EOS is tested for its predictive ability by

**TABLE 12—EXPANSION DATA FOR OIL 4**

DE at 110°F						
$p$ (psig)	$R_s$ (scf/STB)			$B_o$ (RB/STB)		
	Predicted	Adjusted	Experimental	Predicted	Adjusted	Experimental
1,958.0	694.3	694	701	1.3230	1.3243	1.341
1,753.0	694.3	629	633	1.3259	1.2990	1.313
1,557.0	647.9	570	577	1.3086	1.2762	1.291
1,354.0	572.7	509	510	1.2789	1.2524	1.264
1,153.0	500.4	450	450	1.2502	1.2293	1.240
949.0	429.5	391	389	1.2221	1.2063	1.217
748.0	361.5	334	330	1.1952	1.1839	1.193
548.0	295.2	278	270	1.1687	1.1616	1.168
347.0	228.3	220	209	1.1416	1.1382	1.144
157.0	158.4	158	143	1.1120	1.1120	1.116
75.0	121.0	123	106	1.0949	1.0963	1.097
0.0	0.0	000	000	1.0234	1.0234	1.024
DE AT 250°F						
2,547.0	948.5	948	943	1.7692	1.7678	1.671
2,360.0	832.8	863	865	1.6949	1.7168	1.636
2,143.0	758.5	784	788	1.6529	1.6712	1.595
1,893.0	670.6	690	704	1.6017	1.6157	1.553
1,645.0	589.1	604	625	1.5540	1.5644	1.512
1,393.0	511.8	522	548	1.5085	1.5160	1.473
1,150.0	441.6	450	477	1.4667	1.4720	1.436
895.0	371.2	376	407	1.4242	1.4275	1.401
647.0	304.4	307	338	1.3828	1.3846	1.365
400.0	235.9	237	265	1.3383	1.3387	1.326
182.0	163.6	163	190	1.2861	1.2858	1.275
87.0	120.2	120	146	1.2508	1.2504	1.243
0.0	0.0	000	000	1.1241	1.1241	1.094

**TABLE 13—OBSERVED AND PREDICTED DATA, CRUDE OIL 6**

Approach	$p_b$ (psia)	$R_s$ (scf/STB)	$B_{ob}$ (RB/STB)	$\rho$ (lbm/ft <sup>3</sup> )
Experimental	2,746	1,230	1.866	38.0
Coats-Smart	2,398 (-12.7)	1,002 (-19)	1.659 (-11.1)	35.6 (-6.3)
Modified EOS	2,916 (6.2)	1,233 (0)	1.909 (2.3)	37.40 (-1.6)

Numbers in parentheses represent percent error of predictions.

TABLE 14—EXPANSION DATA FOR OIL 6

DE at 234°F						
p (psig)	R <sub>s</sub> (scf/STB)			B <sub>o</sub> (RB/STB)		
	Predicted	Adjusted	Experimental	Predicted	Adjusted	Experimental
2,746.0	1,233.3	1,232	1,230	1.0985	1.9053	1.866
2,598.0	1,071.0	1,142	1,151	1.8030	1.8514	1.821
2,400.0	987.6	1,048	1,059	1.7567	1.7981	1.771
2,200.0	897.9	947	972	1.7051	1.7385	1.725
1,897.0	771.8	806	849	1.6327	1.6562	1.658
1,600.0	662.2	686	737	1.5699	1.5864	1.599
1,300.0	560.2	576	631	1.5112	1.5222	1.543
1,000.0	464.8	474	529	1.4557	1.4624	1.488
700.0	371.6	477	428	1.3999	1.4032	1.433
394.0	271.9	273	321	1.3368	1.3374	1.371
195.0	194.2	194	231	1.2831	1.2826	1.313
112.0	152.2	152	178	1.2516	1.2510	1.274
0.0	0.0	000	000	1.1079	1.1079	1.086

TABLE 15—OBSERVED AND PREDICTED DATA, CRUDE OIL 7

Approach	p <sub>b</sub> (psia)	R <sub>s</sub> (scf/STB)	B <sub>ob</sub> (RB/STB)	ρ (lbm/ft <sup>3</sup> )
Experimental	1,709	557	1.324	44.5
Coats-Smart	1,531 (-10.4)	542 (-2.7)	1.296 (-2.1)	40.7 (-8.5)
Modified EOS	1,572 (-8.0)	624 (12.0)	1.346 (1.7)	45.0 (1.1)

Numbers in parentheses represent percent error of predictions.

a simulating CCE test. Table 7 compares the predicted and adjusted liquid ratio  $V/V_s$  with the observed data. The observed average absolute deviation is 0.156%.

**Crude Oil 2.** This oil is characterized as volatile. The reported bubblepoint pressure,  $p_b$ , is 4,475 psia at 176°F. The predicted values of  $R_s$ ,  $B_{ob}$ , and oil density at the saturation pressure are compared with the experimental data and Coats and Smart's predicted values (their values are based on the original PREOS) in Table 8. Results of simulating DE and CVE tests are fully documented in Table 9 and expressed graphically in Fig. 5. The predicted and adjusted results agree well with the experimental data. The modified EOS, in a predictive mode, reproduced  $R_s$  and  $B_o$  observed data with an average absolute error of 4.9 and 2.26%, respectively. In comparison, Coats and Smart stated that with splitting of the  $C_{7+}$  fraction into three pseudocomponents and regression on nine variables, the original PREOS regenerated  $B_o$  laboratory data with an average deviation of 2.17%.

**Crude Oil 3.** This CO<sub>2</sub>-rich system contains 60 mol% CO<sub>2</sub>. The hydrocarbon system exhibits a saturation pressure and density of 2,612 psia and 44.17 lbm/ft<sup>3</sup> at 180°F. Coats and Smart presented the results of CCE tests on the system at four temperatures. Table 10 gives the observed and predicted saturation pressures and densities at these temperatures with the percentage error for each

property. Examination of tabulated values shows the ability of the proposed expression virtually to duplicate the experimental data.

**Crude Oil 4.** The reported experimental data available on the system includes differential expansion results at 110 and 250°F and CCE data at 110, 180, and 250°F. The system is slightly volatile with  $B_o = 1.671$  and  $R_s = 932$  scf/STB at 250°F. Table 11 lists the predicted values for selected PVT properties compared with the reported values at saturation pressures. Table 12 gives detailed documentation of results of predicting the DE data at the specified temperatures. With adjustment and in terms of the average absolute error, the model predicts  $R_s$  and  $B_o$  data at 110°F within 3.5 and 0.77%, respectively. At 250°F, the equation gives results within 6% for  $R_s$  and 3% for  $B_o$ .

**Crude Oil 6.** This oil exhibits a saturation pressure of 2,746 psia at 234°F. Table 13 gives the reported  $R_s$ ,  $B_o$ , and  $\rho_o$  at the bubblepoint pressure compared with the predicted results. Table 14 shows DE data calculated by the EOS before and after adjustment. (For detailed results of CCE data, see Table 6 of Ref. 20.) In a prediction mode, the modified expression reproduced the entire solution GOR and relative oil volume data with average absolute errors of 6.3 and 1.7%, respectively. (See Table 7 of Ref. 20 for CCE predicted data.)

**Crude Oil 7.** This hydrocarbon system is the least volatile of the oil samples in the Coats and Smart study. The oil shows a bubblepoint of 1,709 psia and a saturation density of 44.5 lbm/ft<sup>3</sup> at

TABLE 16—EXPANSION DATA FOR OIL 7

DE at 131°F						
p (psig)	R <sub>s</sub> (scf/STB)			B <sub>o</sub> (RB/STB)		
	Pred.	Adj.	Exp.	Pred.	Adj.	Exp.
1,694.0	623.5	624	557	1.3464	1.3472	1.324
1,550.0	621.4	587	526	1.3478	1.3321	1.311
1,400.0	581.0	550	493	1.3310	1.3168	1.298
1,252.0	540.3	513	460	1.3139	1.3013	1.285
1,100.0	498.4	475	423	1.2962	1.2853	1.270
950.0	456.9	437	389	1.2786	1.2694	1.256
798.0	414.4	398	349	1.2604	1.2529	1.240
643.0	370.4	358	310	1.2413	1.2357	1.224
500.0	328.8	320	273	1.2231	1.2192	1.209
350.0	283.1	278	229	1.2025	1.2005	1.188
200.0	231.3	230	179	1.1780	1.1779	1.160
102.0	186.5	188	137	1.1551	1.1562	1.136
0.0	0.0	000	000	1.0328	1.0328	1.034

TABLE 17—EXPANSION DATA FOR RED RIVER CRUDE OIL

DE at 250°F						
p (psig)	R <sub>s</sub> (scf/STB)			B <sub>o</sub> (RB/STB)		
	Pred.	Adj.	Exp.	Pred.	Adj.	Exp.
2,377.0	1,060.8	1,060	921	1.8973	1.8947	1.706
2,250.0	933.9	982	872	1.8062	1.8428	1.678
1,950.0	801.3	836	761	1.7242	1.7509	1.614
1,650.0	674.8	698	657	1.6443	1.6622	1.555
1,350.0	561.8	577	561	1.5728	1.5843	1.501
1,050.0	459.5	469	467	1.5076	1.5144	1.448
750.0	361.7	366	375	1.4438	1.4470	1.395
450.0	264.4	266	274	1.3774	1.3780	1.334
225.0	183.0	183	191	1.3175	1.3170	1.279
125.0	139.5	139	140	1.2829	1.2822	1.241
0.0	0.0	000	000	1.1341	1.1341	1.102



131°F. Table 15 shows the predicted PVT properties at saturation pressure compared with the experimental and Coats-Smart model data. Table 16 compares measured DE data with those simulated with the modified PREOS in both predictive and adjusted mode. With adjustment, the average deviations for reproducing the measured data are 7.5% for  $R_s$  and 1.7% for  $B_o$ .

**Red River Crude Oil System.** The crude oil system of the Red River Field (MT) is slightly volatile with  $B_o=1.706$  and  $R_s=921$  at 250°F. The modified equation reproduced the observed  $B_o$  and  $R_s$  with average deviations of 5.1 and 4.3%, respectively. The PVT properties of the crude oil system at saturation pressure were  $p_b=2,392$  psia,  $R_s=921$  scf/STB,  $B_{ob}=1.706$  RB/STB, and  $\rho=38.13$  lbm/ft<sup>3</sup>. Those predicted by the modified EOS were  $p_b=2,497$  psia,  $R_s=1,061$  scf/STB,  $B_{ob}=1.8973$  RB/STB, and  $\rho=36.2$  lbm/ft<sup>3</sup> for errors of 4.4, 15.2, 11.2, and -5.0% for  $p_b$ ,  $R_s$ ,  $B_o$ , and  $\rho$ , respectively. Table 17 gives detailed documentation of simulated DE tests for the system. The equation yields values for  $B_o$  considerably higher than the observed data. The match with the CCE data is generally good.

**Wyoming's Heavy Crude Oil, Teapot Dome Field.** This heavy oil contains 9.61 mol%  $C_1$  and 75.01 mol%  $C_{7+}$ . The plus fraction is characterized by a molecular weight of 223.5 and a specific gravity of 0.8429. The oil exhibits a bubblepoint of 505 psia at 162°F. The PVT properties were  $p_b=505$  psia,  $R_s=110$  scf/STB,  $B_{ob}=1.1098$  RB/STB, and  $\rho=48.77$  lbm/ft<sup>3</sup>. The model predicted  $p_b=520$  psia,  $R_s=113$  scf/STB,  $B_{ob}=1.1060$  RB/STB, and  $\rho=48.77$  lbm/ft<sup>3</sup> with errors of 2.97, 2.7, 0.34, and 0% for  $p_b$ ,  $R_s$ ,  $B_{ob}$ , and  $\rho$ , respectively. Table 18 shows the close match with the reported data.

**North Sea Gas-Condensate System.** The system is characterized by a dewpoint of 6,750 psia at 280°F. The gas contains 73.19 mol%  $C_1$  and 8.21 mol%  $C_{7+}$ . The plus fraction is characterized by a molecular weight of 148 and a specific gravity of 0.16. The maximum liquid dropout with a value of 21.6% occurs at 3,100 psia. Whitson and Torp<sup>10</sup> gave a detailed compositional and experimental analysis of the system. The modified equation predicts a dew-point pressure of 6,189 psia. Table 19 gives complete results of the CVE simulation. The tabulated values show that the EOS pre-

TABLE 18—EXPANSION DATA FOR  
TEAPOT DOME CRUDE OIL

DE at 162°F						
$p$ (psig)	$R_s$ (scf/STB)			$B_o$ (RB/STB)		
	Pred.	Adj.	Exp.	Pred.	Adj.	Exp.
490.3	112.8	113	110	1.1060	1.1060	1.1098
385.3	94.5	97	94	1.0981	1.0991	1.1025
285.3	78.6	80	77	1.0912	1.0920	1.0962
185.3	61.5	63	58	1.0836	1.0840	1.0886
85.3	41.3	42	36	1.0739	1.0740	1.0782
35.3	27.6	28	23	1.0665	1.0665	1.0701
0.0	0.0	00	00	1.0481	1.0481	1.0491

dicts the entire liquid dropout and  $z$ -factor data with average absolute deviations of 4.7 and 1.8%, respectively. Results of the model are generally in excellent agreement with reported data.

## Conclusions

1. Improved correlations for calculating  $a(T_c)$ ,  $b$ , and  $\alpha(T)$  of the plus fraction, methane, and nitrogen are presented.
2. The modified PREOS gives hydrocarbon liquid density predictions that are compatible with, or better than, the S-K and the A-K density correlations.
3. The proposed modifications eliminate the need for splitting the heptanes-plus fraction into pseudocomponents.
4. The proposed modifications significantly improve the ability of the PREOS to predict the PVT properties of complex hydrocarbon mixtures.
5. With such significant improvement in the predictive capability of the modified EOS, the equation is recommended for calculating the volumetric behavior of crude oil and condensate systems.

## Nomenclature

$a, b, A, B$  = EOS constants

$B_o$  = oil FVF obtained from differential expansion, RB/STB

$B_{ob}$  = oil FVF at bubblepoint pressure, RB/STB

TABLE 19—CVE AT 280°F FOR THE NORTH SEA RESERVOIR

	Pressure (psig)							
Component	6,750.0	5,500.0	4,300.0	3,100.0	2,100.0	1,200.0	700.0	700.0*
CO <sub>2</sub>	0.02370	0.02379	0.02399	0.02438	0.02493	0.02568	0.02630	0.00748
N <sub>2</sub>	0.00310	0.00320	0.00327	0.00334	0.00338	0.00337	0.00332	0.00037
C <sub>1</sub>	0.73190	0.75710	0.77263	0.78619	0.79345	0.79296	0.78412	0.10353
C <sub>2</sub>	0.07800	0.07950	0.08034	0.08126	0.08227	0.08376	0.08523	0.02357
C <sub>3</sub>	0.03550	0.03574	0.03577	0.03585	0.03619	0.03730	0.03903	0.01904
i-C <sub>4</sub>	0.00710	0.00706	0.00700	0.00694	0.00696	0.00721	0.00774	0.00600
n-C <sub>4</sub>	0.01450	0.01426	0.01403	0.01381	0.01379	0.01438	0.01570	0.01572
i-C <sub>5</sub>	0.00640	0.00620	0.00601	0.00580	0.00569	0.00590	0.00659	0.01079
n-C <sub>5</sub>	0.00680	0.00652	0.00627	0.00600	0.00583	0.00604	0.00682	0.01355
C <sub>6</sub>	0.01090	0.01023	0.00964	0.00893	0.00839	0.00847	0.00966	0.03245
C <sub>7+</sub>	0.08210	0.05641	0.04105	0.02749	0.01912	0.01492	0.01549	0.76750
	z Factor							
Adjusted	1.2633	1.1052	0.9962	0.9253	0.9039	0.9186	0.9409	
Experimental	1.2380	1.0890	0.9720	0.9130	0.9140	0.9370	0.9600	
Predicted	1.2618	1.1105	0.9958	0.9239	0.9029	0.9182	0.9407	
	G <sub>p</sub> (%)							
Adjusted	0.00000	9.797	22.045	38.2377	54.817	71.399	80.830	
Experimental	0.00000	9.024	21.744	38.674	55.686	72.146	81.301	
Predicted	0.00000	9.512	21.782	38.093	54.800	71.473	80.940	
	Liquid Dropout (%)							
Adjusted	0.0	15.84	19.98	21.33	20.92	19.61	18.51	
Experimental	0.0	14.10	19.70	21.60	21.30	20.20	19.30	
Predicted	0.0	12.89	19.07	20.92	20.56	19.23	18.13	
*Residual liquid composition.								

\*Residual liquid composition.

## Author



**Tarek Ahmed**, the Union Pacific Resources Professor at Montana Tech in Butte, MT, is the author of a recent textbook, *Hydrocarbon Phase Behavior*. He has research interests in reservoir modeling, phase equilibrium, and EOR. He holds a PhD degree in petroleum engineering from the U. of Oklahoma.

$f_L$  = volume fraction of liquid in expansion cell  
 $G_p$  = volume fraction of gas removed from a laboratory CVE cell  
 $k_{ij}$  = binary interaction coefficient between Components  $i$  and  $j$   
 $m$  = characteristic constant  
 $M$  = molecular weight, lbm/lbm mol  
 $p$  = pressure, psi  
 $p_b$  = bubblepoint pressure, psi  
 $p_c$  = critical pressure, psi  
 $p_s$  = saturation pressure, psi  
 $R$  = universal gas constant, 10.73 psia-ft<sup>3</sup>/mol-°R  
 $R_s$  = solution GOR obtained from differential expansion, scf/STB  
 $T$  = temperature, °F or °R  
 $T_c$  = critical temperature, °R  
 $V$  = laboratory-expansion-cell total volume, ft<sup>3</sup>  
 $V_L$  = volume of liquid in expansion cell, ft<sup>3</sup>  
 $V_m$  = molar volume  
 $V_s$  = volume of expansion cell at saturation pressure, ft<sup>3</sup>  
 $x$  = mole fraction  
 $z$  = compressibility factor  
 $\alpha$  = correction factor for  $a$   
 $\gamma$  = specific gravity  
 $\rho$  = density, lbm/ft<sup>3</sup>  
 $\rho_{ob}$  = density at bubblepoint, lbm/ft<sup>3</sup>  
 $\omega$  = acentric factor  
 $\Omega_a, \Omega_b$  = EOS constants

## Subscripts

$c$  = critical  
 $i, j$  = component number  
mix = mixture  
 $o$  = oil  
 $ob$  = bubblepoint

## References

1. van der Waals, J.D.: "On the Continuity of the Liquid and Gaseous State," PhD dissertation, Sigthoff U., Leiden (1873).

2. Peng, D.Y. and Robinson, D.B.: "A New Two-Constant Equation of State," *Ind. & Eng. Chem.* (1976) **15**, No. 1, 59-64.
3. Soave, G.: "Equilibrium Constants From a Modified Redlich-Kwong Equation of State," *Chem. Eng. Sci.* (1972) **27**, 1197-1203.
4. Coats, K.H. and Smart, G.T.: "Application of a Regression-Based EOS PVT Program to Laboratory Data," *SPE* (May 1986) 277-99.
5. Wilson, A., Maddox, R.N., and Erbar, J.H.: "C Fractions Affect Phase Behavior," *Oil & Gas J.* (Aug. 21, 1978) 76-81.
6. Katz, D.L. and Firoozabadi, A.: "Predicting Phase Behavior of Condensate/Crude-Oil Systems Using Methane Interaction Coefficients," *JPT* (Nov. 1978) 1649-55; *Trans.*, AIME, **265**.
7. Firoozabadi, A., Hekim, Y., and Katz, D.L.: "Reservoir Depletion Calculations for Gas Condensates Using Extended Analyses in the Peng-Robinson Equation of State," *Cdn. J. Chem. Eng.* (1978) **56**, 610-15.
8. Yarborough, L.: "Application of a Generalized Equation of State to Petroleum Reservoir Fluids," *Equations of State in Engineering, Advances in Chemistry Series*, K.C. Chao and R.L. Robinson (eds.), American Chemical Soc., Washington, DC (1979) **182**, 385-435.
9. Whitson, C.H.: "Characterizing Hydrocarbon Plus Fractions," *SPEJ* (Aug. 1983) 683-94.
10. Whitson, C.H. and Torp, S.B.: "Evaluating Constant-Volume Depletion Data," *JPT* (March 1983) 610-20.
11. Lohrenz, J., Bray, B.G., and Clark, C.R.: "Calculating Viscosities of Reservoir Fluids From Their Compositions," *JPT* (Oct. 1964) 1171-76; *Trans.*, AIME, **231**.
12. Katz, D.L.: "Overview of Phase Behavior in Oil and Gas Production," *JPT* (June 1983) 1205-14.
13. Ahmed, T., Cady, G., and Story, A.: "An Accurate Method of Extending the Analysis of C<sub>7+</sub>," paper SPE 12916 presented at the 1984 SPE Rocky Mountain Regional Meeting, Casper, WY, May 21-23.
14. Ahmed, T., Cady, G., and Story, A.: "A Generalized Correlation for Characterizing the Hydrocarbon Heavy Fractions," paper SPE 14266 presented at the 1985 SPE Annual Technical Conference and Exhibition, Las Vegas, Sept. 22-25.
15. Kenyon, D. and Behie, G.: "Third SPE Comparative Solution Project: Gas Cycling of Retrograde Condensate Reservoirs," *JPT* (Aug. 1987) 981-97.
16. Riazi, M.R. and Daubert, T.E.: "Characterization Parameter for Petroleum Fractions," *Ind. & Eng. Chem. Res.* (1987) **26**, No. 4.
17. Petersen, C.S.: "A Systematic and Consistent Approach To Determine Binary Interaction Coefficients for the Peng-Robinson Equation of State," *SPE* (Nov. 1989) 488-96.
18. Standing, M.B. and Katz, D.L.: "Density of Crude Oils Saturated With Natural Gas," *Trans.*, AIME (1942) **146**, 159-65.
19. Alani, G.H. and Kennedy, H.T.: "Volumes of Liquid Hydrocarbons at High Temperatures and Pressures," *Trans.*, AIME (1960) **219**, 288-92.
20. Ahmed, T.: "Supplement to A Practical Equation of State," SPE 22219 available from SPE Book Order Dept., Richardson, TX.

## SI Metric Conversion Factors

bbl	× 1.589 873	E-01	= m <sup>3</sup>
ft <sup>3</sup>	× 2.831 685	E-02	= m <sup>3</sup>
°F	(°F - 32)/1.8		= °C
lbm	× 4.535 924	E-01	= kg
psi	× 6.894 757	E+00	= kPa

## SPE

Original SPE manuscript received for review Nov. 2, 1988. Paper accepted for publication Sept. 17, 1990. Revised manuscript received July 25, 1990. Paper (SPE 18532) first presented at the 1988 SPE Eastern Regional Meeting held in Charleston, NC, Nov. 1-4.